



FFI-rapport 2013/00524

Change detection in SAR-images from the TerraSAR-X satellite with main focus towards harbors and container terminals



Terje Johnsen



Change detection in SAR-images from the TerraSAR-X satellite with main focus towards harbors and container terminals

Terje Johnsen

Norwegian Defence Research Establishment (FFI)

1 October 2013

FFI-rapport 2013/00524

1158

P: ISBN 978-82-464-2300-5

E: ISBN 978-82-464-2301-2

Keywords

Radar

SAR

Endringsdeteksjon

Approved by

Trygve Sparr

Project Manager

Johnny Bardal

Director

English summary

The detection of changes or no change in a set of images of the same scene recorded at different times is of importance in many applications. The time scale could be from seconds to days or months. Man-made constructions often contain regions with high scattering from radar waves that are readily detected. The use of Non-Coherent Change Detection (NCCD) from intensity images or additionally using the phase information in the complex SAR images in a Coherent Change Detection (CCD) are powerful techniques that can detect changes and even repositioning of objects in almost the same position. This report presents results using both techniques based on satellite SAR images. This exemplifies what can also be obtained by an airborne platform with proper control of radar and navigation.

Based on two high resolution satellite images recorded of the Oslo harbor region analysis has been performed to extract information of changes. The two images were recorded with 11 days interval and were co-registered to a fraction of a pixel. The high quality of these images represent an example of what would be the best performance obtainable given that precise control are available in an airborne SAR platform. Analyses have been performed for NCCD and CCD in the two images. Different objects have been studied with a detailed analysis of container terminals and what information could be extracted from such objects. Simulations of SAR images using modeled containers in different stacking configurations are also used to help understand the backscattered response from containers. Based on this knowledge, changes to container stacking configurations were extracted from the images. A coloring scheme was applied to easier extract changes in the CCD analysis. The two magnitude images and the coherence measure from the CCD calculations were used in the R, G and B channel of an image, respectively. Objects only present on day 1 or 2 respectively appear as red or green colored objects. An object with high backscattering that are unchanged from day 1 to day 2 and that result in high coherence will appear as white. A series of objects are presented that show how these techniques can provide powerful tools for change detection.

Sammendrag

Deteksjon av om det er endring eller ikke i et sett av bilder tatt ved ulike tider er viktig i mange anvendelser. Tidsskalaen kan være fra sekunder til dager eller måneder. Menneskelagde konstruksjoner har ofte områder som gir kraftig tilbakespredning fra radarbølger som lett lar seg detektere. Bruken av ikke-koherent endringsdeteksjon på intensitetsbilder eller i tillegg å benytte fasen i det komplekse SAR-bildet i en koherent endringsdeteksjon utgjør kraftige teknikker som kan detektere endringer og til og med reposisjonering i nesten samme posisjon. Denne rapporten presenterer resultater hvor begge teknikker er brukt på SAR-bilder fra satellitt. Dette som et eksempel på hva en også kan oppnå fra en flybåren plattform med god kontroll på radar og navigasjon.

To høyoppløselige SAR-bilder ble tatt opp over Oslo havn og områdene rundt fra TerraSAR-Xsatellitten. Bildene ble tatt med 11 dagers mellomrom og er benyttet i forbindelse med analyse av endring i scenen. Bildene er av høy kvalitet og metoder for samregistrering med en nøyaktighet på en brøkdel av pikselstørrelsen ble benyttet. Den høye kvaliteten representerer et eksempel på hva en maksimalt kan oppnå også fra en flygende plattform gitt at en har tilstrekkelig nøyaktig kontroll. Analyser ble utført for koherent og ikke-koherent endringsdeteksjon i bildene. Forskjellige objekter har blitt adressert med hovedfokus på containerterminaler og hvilken informasjon en kan trekke ut fra disse. I denne forbindelse ble det simulert SAR-bilder basert på input fra CAD modeller av containere for å bedre kunne tolke tilbakespredningen fra disse i de virkelige SAR-bildene. Endringer i stablingen av containere var ofte mulig å kvantisere gjennom analysene. I forbindelse med visualiseringen av beregningene for koherent endringsdeteksjon ble det benyttet en fargekoding av bildene. De to opprinnelige amplitudebildene samt den beregnede koherensen i hvert pikselelement ble lagt inn i henholdsvis R, G og B-kanalen i et bilde. Objekter som er tilstedeværende kun dag 1 eller dag 2 har lav koherens og fremkommer som henholdsvis røde eller grønne objekter. Faste objekter med høy tilbakespredning og som har høy koherens fremkommer som hvite i bildet. En rekke objekter av ulik type blir presentert for å vise at disse teknikkene kan bidra med kraftige verktøy for deteksjon av endringer.

Contents

1	Introduction	7
2	Change detection	8
2.1	Non-coherent change detection	10
2.2	Coherent change detection	10
3	Case study: Change detection in container terminals	12
3.1	Container terminals	12
3.2	SAR image of container terminal 1	13
3.3	Analysis of scattering patterns from containers	14
3.3.1	Analysis of basic stacked container configurations	14
3.3.2	Analysis of complex stacking configuration	18
3.4	Non-coherent change detection in the container terminal 1 images	19
3.4.1	Analysis of cluster configuration	19
4	Coherent change detection (CCD)	22
4.1	Coherent change detection results	23
4.1.1	Various objects observed close to the harbor area	23
4.1.2	Result from container terminal analysis	27
5	Conclusions	31
	Referenses	32

1 Introduction

The detection of changes or no change in a set of images of the same scene is of importance in a large variety of situations. The time scale could be from seconds to days or months dependent on application. In detecting changes, two or more images must be recorded of the same scene at different times. Images can be of many different sources, such as optical, multi-spectral or radar SAR images. In this report we focus on radar SAR images and results related to change detection from a series of SAR images.

Man-made constructions often contain regions of high scattering that are readily detected by radar. Changes in constructions or movements resulting in scattering regions reappearing in new positions or change their magnitude are candidates for successful application of change detection algorithms. The probability of detecting a change will depend on factors such as recording geometry similarities for the images, radar stability and pixel positional accuracy. The appearing or disappearing of a scatterer in a homogeneous background are more readily detected than scattering changes in a dense scatterer environment as found in a city. Objects with low backscattering levels or objects with low contrast towards background are less likely detected by change detection. Use of intensity information for non-coherent detection or the more sensitive phase information in a coherent change detection scheme will be applied to selected scenes.

Our group at FFI has an X-band SAR radar named PicoSAR which has led to interest in change detection in SAR images. We normally operate it from a helicopter and it could be used for producing images for change detection purposes. During a cooperating trial with other projects at FFI we recorded SAR images both with PicoSAR and from the TerraSAR-X satellite at the same time. Two different days with an interval of 11 days were used as recording dates. The satellite has a very high quality in control of satellite orbit, timing and recording geometry and will produce SAR images that can be viewed as a very good basis for extracting information after a change detection process. Analysis of images from the satellite has therefore been used to obtain a measure of what can be possible in the future from SAR sensors at airborne platforms given sufficient control and accuracy of beam and navigation.

The images from TerraSAR-X were taken over Oslo harbor and part of town area as shown in Figure 1.1. The images show a large variety of objects but a major part of this report will focus on the harbor area and a depth study of change detection details within container terminals as a case study.

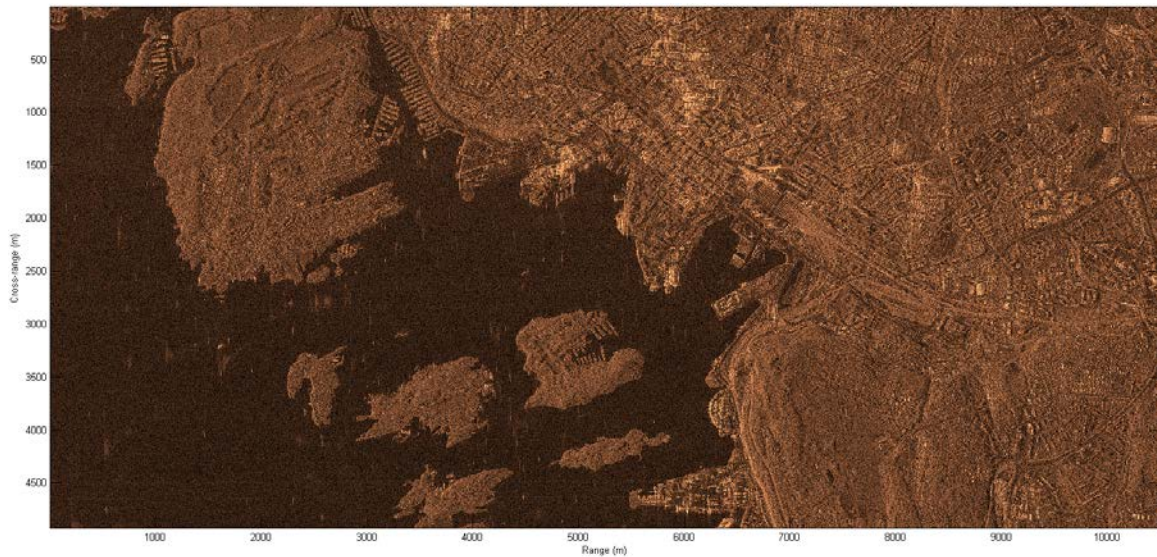


Figure 1.1 Image from TerraSAR-X with about 6000*12000 pixels and a sub-meter resolution.

2 Change detection

In detecting changes the whole image as shown in Figure 1.1 represents a suitable scale for detecting large scale changes in a manual process. In the higher scale images of Figure 2.1 and Figure 2.2 one can visually easily spot larger changes as pointed out in the boat positions labeled with red circles. In an eleven days period the number of changes in a scene like this is enormous as will be seen in this report. Manually inspection of a pair of images can give valuable information but it is time consuming. If one can implement automatically comparison or semi-automatically processes that can draw attention to areas of interest it is believed that the number of changes that can be detected will increase.

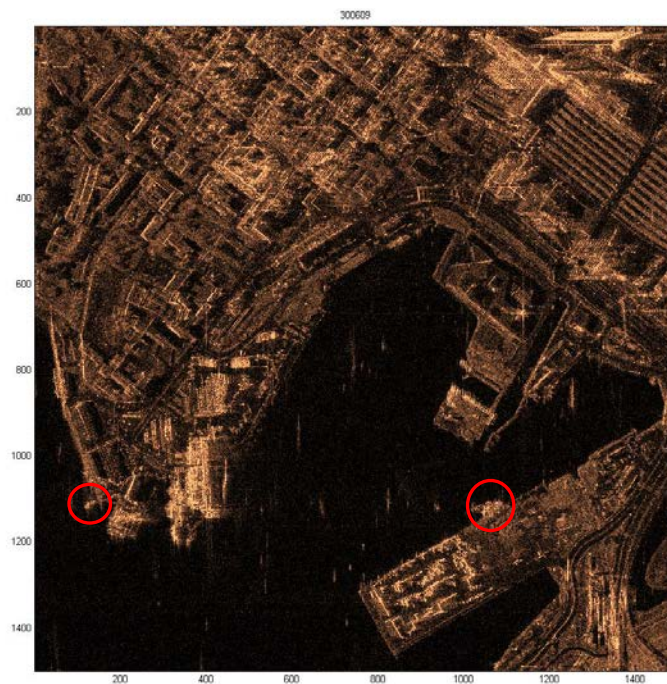


Figure 2.1 A smaller section of the SAR image for day 1

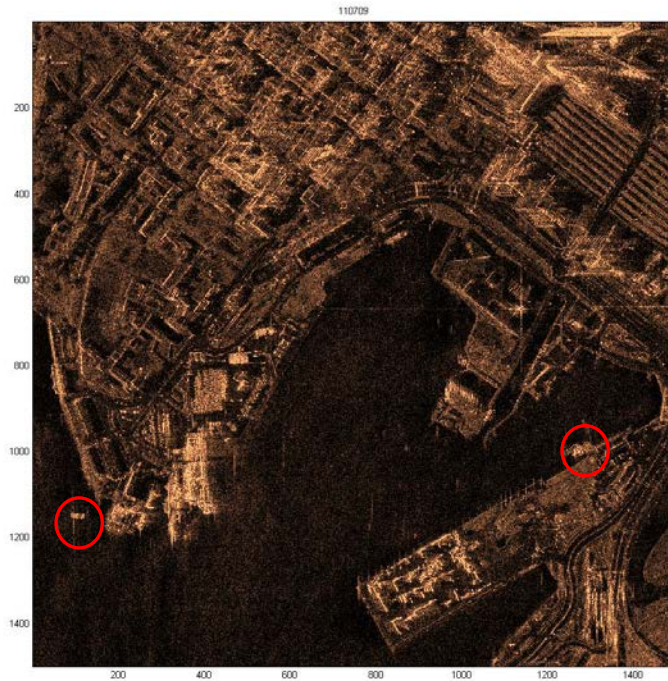


Figure 2.2 A smaller section of the SAR image for day 2

To be able to automatically search for changes in two images their registration must be as good as possible. The recording geometry with a grazing angle of 60 degrees was kept unchanged and simultaneous ground truth registration was captured. The two images were co-registered by use of common corner reflectors as shown within red circles in Figure 2.3. Methods were used to co-register pixels within a fraction of a pixel.

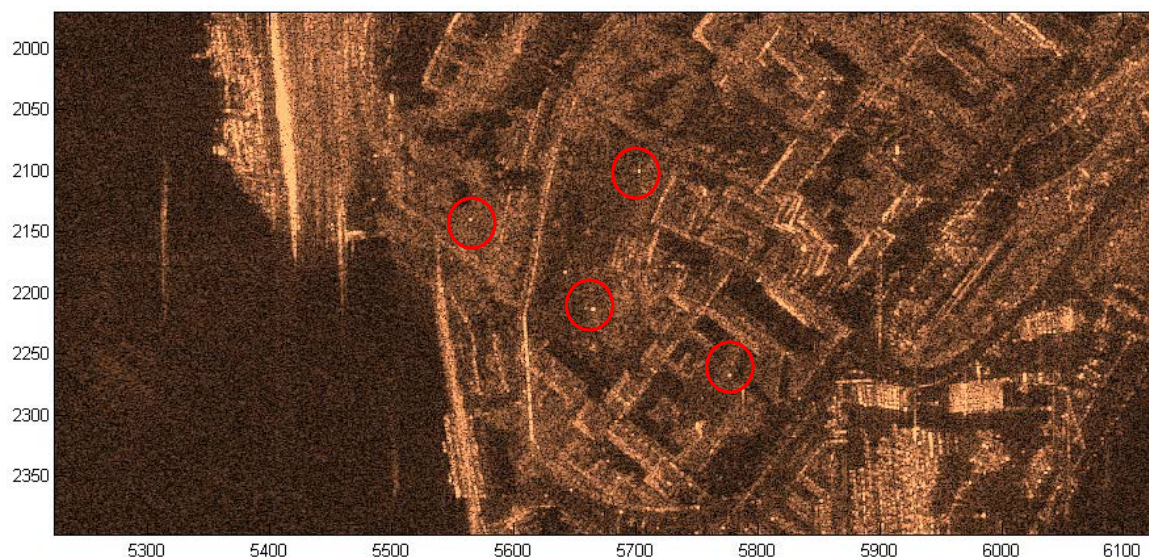


Figure 2.3 Part of scene containing reflectors for better co-registration

Change detection and characterization of man-made objects in rural areas from SAR images have been addressed in many publications [1]-[7]. They cover a broad range from identification of

building heights using shadows, multi-aspect view analysis of buildings to step changes in RCS and moving object detection by investigation of changes in series of images to mention a few. The containers can be viewed in many cases as a simpler problem where all objects have similarities in characteristics but complicating factors of dense packing and large variation in stacking configuration that introduces challenges.

2.1 Non-coherent change detection

In Non-coherent change detection (NCCD) in radar, one compares intensity images formed by calculating the absolute value of the originally complex SAR image. As shown in Figure 2.4, the dynamics often shows sharply defined regions of high intensity reflectivity close to low intensity regions. The co-registration of pixels must therefore be of high precision to ensure optimal performance in change detection calculations. The presence of speckle noise in images has led to often using some averaging region to provide a more robust measure of the mean backscatter intensity. Other analysis could use statistics measures or ratios to provide change detection. In section 3.4 the method selected for our analysis is described in more detail.



Figure 2.4 Section of a city scene showing details on a fine scale.

2.2 Coherent change detection

Coherent change detection (CCD) utilizes the additional phase information incorporated within the complex SAR image. The two high resolution TerraSAR-X images with equal recording geometry have been co-registered to a high precision as a prerequisite for change detection analysis. A measure of similarity between the complex SAR images will be presented from calculations using the measure of sample coherence [11] defined as

$$\hat{\gamma} = \frac{\left| \sum_{k=1}^N f_k g_k^* \right|}{\sqrt{\sum_{k=1}^N |f_k|^2 \sum_{k=1}^N |g_k|^2}}, \quad (1)$$

where f and g are the complex SAR images of the scene for day 1 and 2 indexed at pixel k and $*$ is the complex conjugate. The measure is an average measure of similarity calculated over a

sliding window of area size N pixels and geometry (n,m) . The output values are in the interval 0 to 1, where a value of 1 indicates perfect coherence. In Figure 2.5 the sample coherence has been calculated for three different window sizes 3x3, 5x5 and 9x9 seen from top left to bottom for one of the container terminals. The highest resolution calculation (top left) results in a coherence image that distinguishes small changes most accurately, but it also has the highest noise apparent look from the presence of local high coherence pixels spread out in the image. In the lowest resolution calculation of 9x9 (bottom), the noise looking response is smoothed to a much higher degree but the window size is large compared to the width of containers which will be used as a case study. This results in averaging over several containers. As a compromise a window size of 5x5 (top right) is used in these analysis. Here, sufficient suppression of the noise like contribution is achieved while not smoothing out container contribution severely.

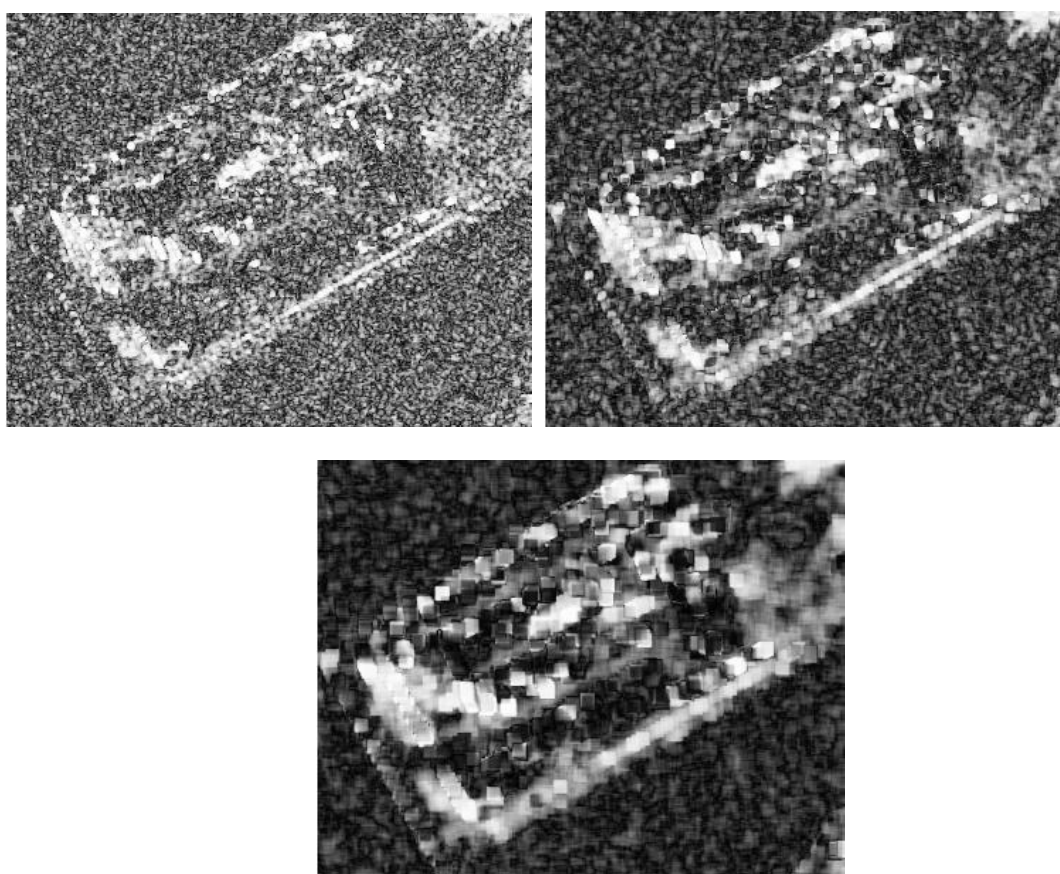


Figure 2.5 Sample coherence calculations from container terminal 1 using window sizes of 3x3, 5x5 and 9x9 from top left to bottom, respectively.

3 Case study: Change detection in container terminals

In this report, container terminals in the Oslo harbor are selected as a case study of change detection. The analyses are divided in a NCCD and a CCD section. To understand which parts of the container that contributes to the bright scattering regions and to be able to extract quantitative information of containers and stacking configuration and changes to the container stacks, simulations have also been used with modeled containers from a CAD tool and a SAR simulation tool (MOCEM LT).

3.1 Container terminals

Container harbors are constantly changing as containers are loaded on or off ships or reorganized in their stacking configuration. There is not one single type of container, but a common set of sizes are used with typical lengths of 20, 40, 45, 48 and 53 foot. In addition they are produced in two heights: standard and high. Containers are often stored in a flat area in large numbers as shown in Figure 3.1. They consist of a rather uniform set of objects piled up in stacks forming densely packed clusters that can take on a large variation in stack height, orientation and area coverage. Clusters can also contain stacks of different container sizes. In the harbor under study, clusters of containers are ordered such as to get easy access to containers. Within each cluster, container stacks are oriented with their long sides parallel or perpendicular to each other. Often, stacks of same orientation and height can form a flat top surfaced block structure. In most cases the clusters grow or shrink on the perimeter, maintaining a constant height in its interior. Stairs of various heights are therefore found mainly at the outskirts.



Figure 3.1 Different stacking configurations of containers here in a view of terminal 2

In satellite SAR images containers can be observed, but detailed quantitative information of the number of containers and their stacking geometry can be difficult to extract. Different orientations of containers result in unequal appearances in the SAR images. This section of the report investigates the possibility of extracting orientation and detailed stacking configuration from recorded TerraSAR-X SAR images in conjunction with non-coherent change detection. To properly understand the SAR images resulting from different stacking configurations, a set of simple stacks of containers are initially studied to establish necessary knowledge of typical scattering and layover effects. To further understand the appearance of strong scatterers in the

SAR images, simulations of SAR images by use of MOCEM LT and 3D models of containers are applied. MOCEM is a component of SIROS, the DGA (part of French MoD) high resolution SAR image simulator. MOCEM LT generates images from CAD models as explained by C. Cochin et al in reference [8].

3.2 SAR image of container terminal 1

SAR images of a container terminal labeled 1 in Oslo harbor have been recorded from the TerraSAR-X satellite at two different dates as shown in Figure 3.2 and Figure 3.3.

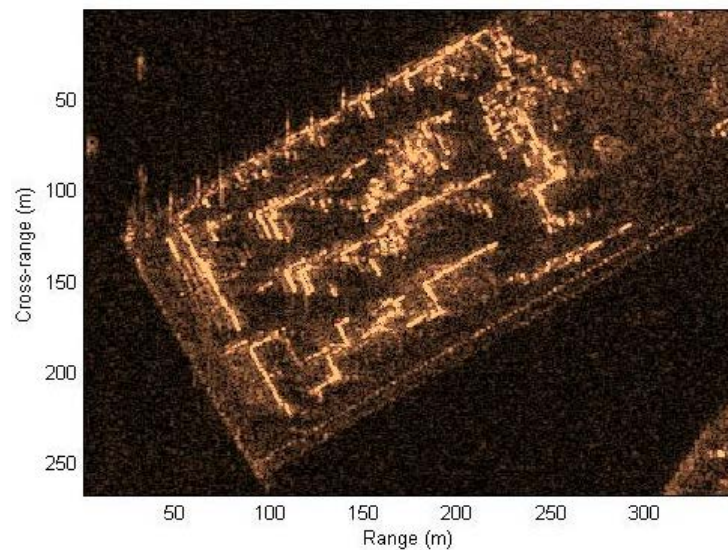


Figure 3.2 Container terminal 1 on day 1

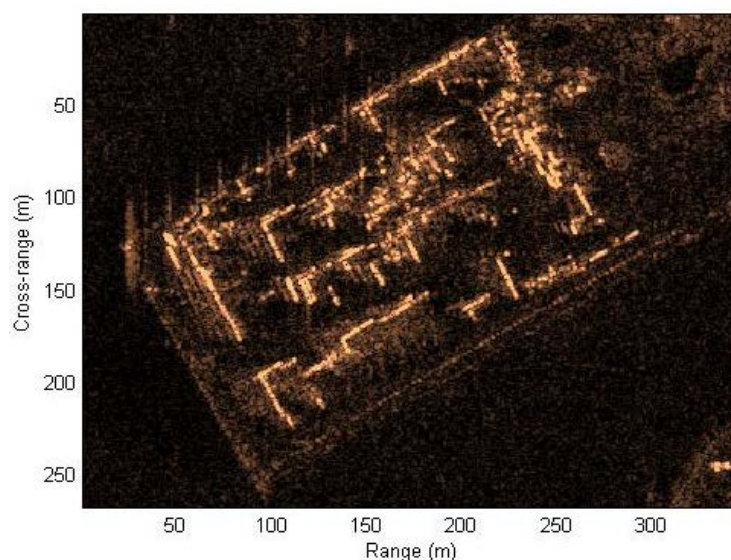


Figure 3.3 Container terminal 1 on day 2

3.3 Analysis of scattering patterns from containers

To better understand the scattering patterns observed from container clusters, a simple generic container model is built, as shown in Figure 3.4. All sides of the model have the same ribbed pattern with beams forming the skeleton that these side walls are connected to. The CAD model has a simplified structure where all small and large rectangles meet at right angles. In real containers, not all edges are right angled but a larger spread in the structure is found as shown in Figure 3.5. The model therefore gives rise to trihedral corner reflectors where the top of the bottom beam represent one of the sides. From the real images it is observed that the angles often form dihedral corner reflectors with the bottom beam.



Figure 3.4 Model of a 40 foot standard height container with a detailed view to the left.

These have a lower radar cross section than the trihedral reflectors [9] but still represent a strong scattering center. Despite this imperfection, the model visualizes the main contributing structures to the observed scattering patterns.

Some of the main scattering regions are found to be located in the crossover region along the bottom side of the wall towards the bottom beam as shown in Figure 3.5 when the angle of incidence is not at right angle relative to the container facets. This will be named wall-beam scattering in the following. Another major region will be the two bounce scattering with the ribbed pattern of the walls and the harbor ground named wall-ground scattering.



Figure 3.5 Different structures found on real containers. The two left images are most common.

3.3.1 Analysis of basic stacked container configurations

Figure 3.6 (left) shows a CAD model where two shipping containers are stacked on top of each other. Simulating the resulting SAR image by use of MOCEM LT produces the image shown to the right in Figure 3.6. To understand the SAR image and the folding phenomena that are observed, Figure 3.7 illustrates where the identified scattering points, drawn in red, end up in the SAR imaging plane parallel to the base of the container stacks.

The grazing angle α of the sensor pointing vector determines the folding parameters. Scattering centers at height h will be mapped to the image plane at a distance x in the direction of the radar given by

$$x = h \tan \alpha \quad (1)$$

The orientation angle β of the container in azimuth relative to the observation vector will result in a shifted scattering pattern from the contour of the stack. In Figure 3.8, a two container stack produces a folded scattering pattern resulting from the bottom-beam of the top container in the stack. This appears shifted along both axes as the dotted line shows. This explains the SAR image shown to the right in Figure 3.6. The upper L-formed pattern results from wall-ground scattering and this produces a strong reflection. The lower L-form, appearing at a shorter range, is the folded scattering response from the wall-beam shown in Figure 3.5.

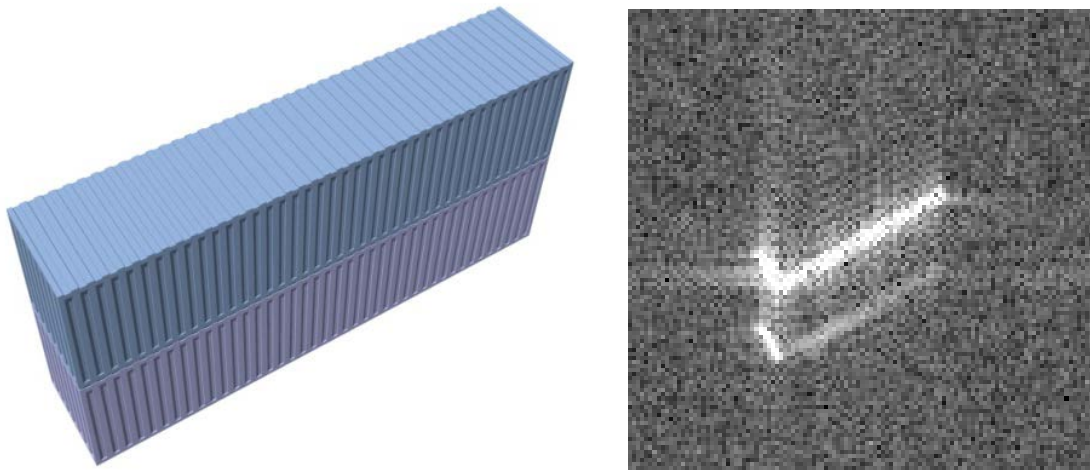


Figure 3.6 Left: A CAD model with a stack of two containers. Right: Simulated SAR image with the CAD model to the left as input and the SAR sensor in the position of the reader.

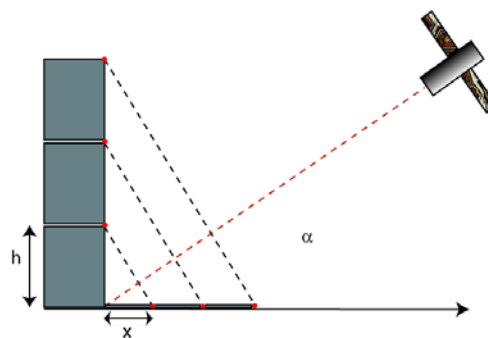


Figure 3.7 Illustration of folding geometry of scatterers

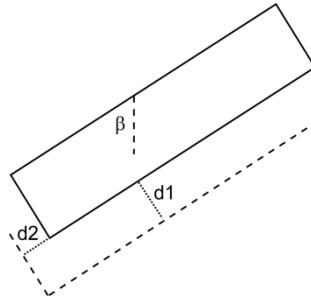


Figure 3.8 The dotted line illustrates the displaced appearance of scattering response due to folding from the bottom of the second container in the stack. The separation of short side and long side lines named $d1$ and $d2$ depends on container orientation angle β .

The distances $d1$ and $d2$ in Figure 3.8 represent separation between lines that appear in the SAR images and can be written as

$$\begin{aligned} d1 &= h \tan(\alpha) \sin(\beta) \\ d2 &= h \tan(\alpha) \cos(\beta) \end{aligned} \quad (2)$$

A lower grazing angle results in less spacing of container reflection lines $d1$ and $d2$ which can disable the possibility of determining the number of stacked containers in the vertical direction. Dependent on azimuth viewing angle β either the short or the long sides wall-beam scatterers of the container stack will be more separated.

In addition to stacks of equal height, edge areas with stairs of different sizes are frequently observed as seen in Figure 3.1. Figure 3.9 shows a step cluster of containers where regions generating wall-roof scattering are drawn in red. The scattering mechanisms will be similar to wall-ground scattering and will result in strong scattering due to metal on both bouncing sides. To distinguish wall-roof scattering from stairs and wall-beam scattering from ordinary stacks in height, the scattering patterns from stairs are plotted for different incidence angles in Figure 3.10. The radar sensor is viewing the stairs at an azimuth angle of 45 degrees and the plot shows the folding of scattering patterns viewed in the image plane. The four blue solid lines represent the position of these scattering lines in true range position. When the grazing angle is changed from 30 to 70 degrees in a 10 degrees interval, the resulting folded scattering pattern is as drawn with dotted lines and color red, black, green, magenta and blue, respectively. As expected, the folded lines will be folded closer to the solid lines for small grazing angles. As the angle increases, the distances between the lines decrease until they for a given angle collapse at the position of the first blue line representing the wall-ground scattering region. As the angle is further increased, the distance interval increases, but the sequence of folded lines is reversed. The upper stair steps wall-roof folding line appears at the shortest range.

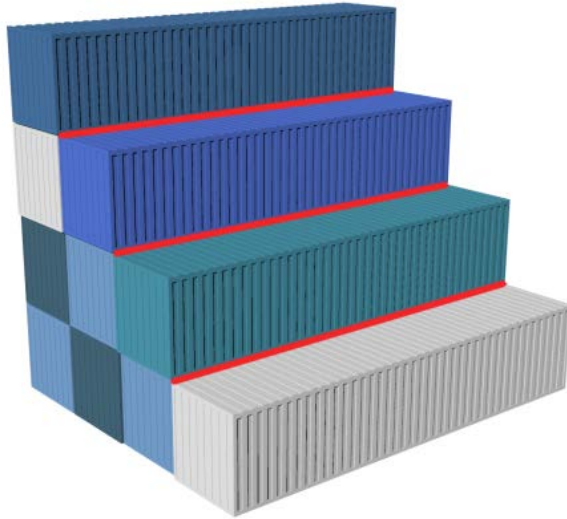


Figure 3.9 Example of stair stacking configuration often localized to the edge of container clusters

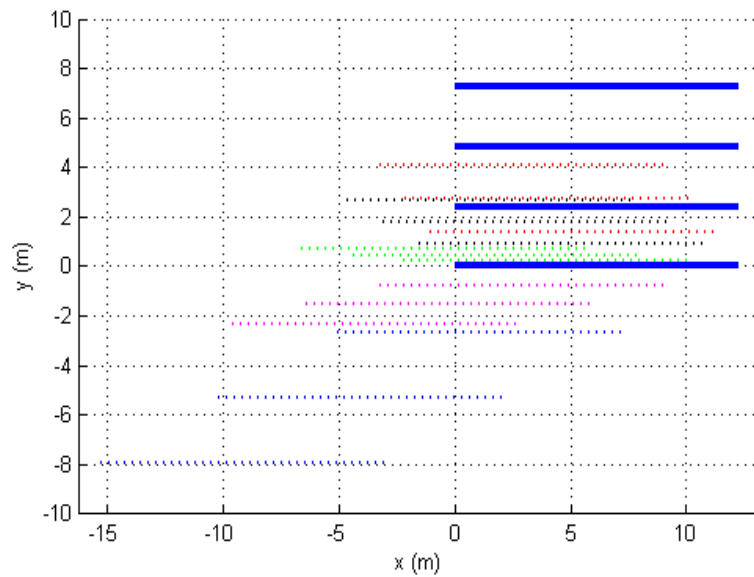


Figure 3.10 Scattering from the wall-roof scattering regions of the stair in Figure 3.9 is shown for grazing angles 30, 40, 50, 60 and 70 degrees drawn with dotted lines and color red, black, green, magenta and blue, respectively. The azimuth viewing angle is 45 degrees.

For all of these folded scattering lines, the endpoints will be shifted only in range. Since different scattering centers are located at separate ranges in the container cluster, their endpoints will generally not be lined up along the same cross-range except for at an azimuth angle equal to zero. Knowledge of the satellite and scene geometry then enables us to distinguish between ordinary stacks of containers and stairs in a stacked cluster and determining the configuration in many cases.

3.3.2 Analysis of complex stacking configuration

In Figure 3.11, an example of a more complex stacking configuration is shown where different stacks have different heights and part of the cluster contains a stair.

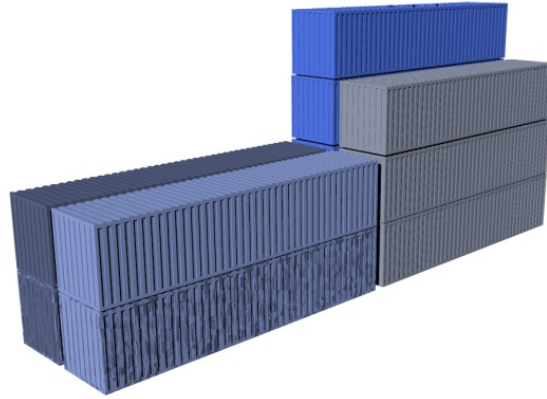


Figure 3.11 Example of a complex stacking configuration

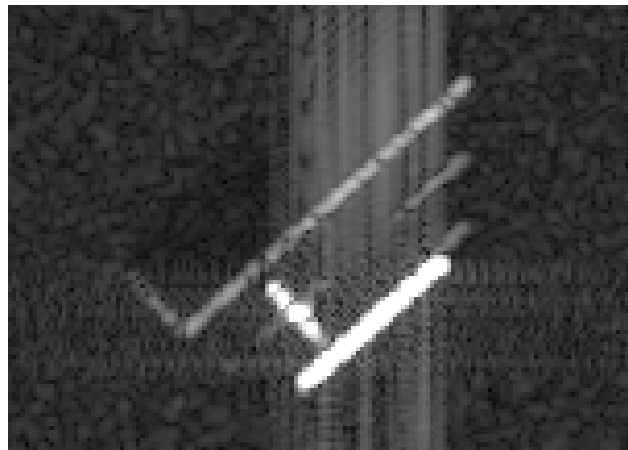


Figure 3.12 Simulated SAR image by use of MOCEM LT from the container configuration shown in Figure 3.11.

The resulting SAR image produced by use of MOCEM LT is shown in Figure 3.12. The two most intense scattering regions represent scattering from the wall-roof from the short-side of level 3 and the long-side of level 4 seen in Figure 3.11. The large upper L-form represents scattering from the wall-ground of the whole cluster. This is similar to what was observed in Figure 3.6 but with longer sides due to the configuration. In addition, wall-beam scattering are found in between with a lower intensity. The closest of these lines as seen by the radar are partly indistinguishable by the longest wall-roof response. The wall-roof long-side scattering region has endpoints to the right that are shifted in cross-range relative to the wall-beam and wall-ground lines and therefore represent a stair configuration as exemplified from Figure 3.10. Indication of a stair can also be found from the difference in long side distance dI of this lowest high scattering response line compared to the other parallel lines of equal distance.

3.4 Non-coherent change detection in the container terminal 1 images

To identify regions of change a non-coherent change detection scheme is applied. The applied procedure initially smooths the two images to attenuate speckle and small patches of strong response. Predominant scattering regions in the images in Figure 3.2 and Figure 3.3 from the containers show a high intensity. To extract the regions of major change related to containers, binary images are first formed by use of threshold-values that extract regions of high backscattering. By further subtraction, difference images are produced for further processing. In these, regions that are changed and those that remain unchanged by this threshold level are labeled.

To further refine the map of detected changes, morphological functions were applied. First, dilation followed by erosion was computed on a 3x3 pixel size to close small gaps. The container scattering is identified by straight line segments of defined lengths given by the orientation of the containers relative to the radar. A morphological function that removes pixels from the border of the objects without allowing the objects to break apart results in a skeleton of the image that is suitable to identify line segments representing edge scattering. The final difference images are dilated to form more extended regions comparable to what is observed in the original image followed by an island function identifying connected scattering regions. The smallest islands were removed due to the knowledge of a smallest size representing short side scattering. In Figure 3.13, the resulting regions of high scattering intensity uniquely found on day 1 and 2 are drawn blue and red, respectively. Unchanged areas are shown with original colors. This directs closer attention towards areas of interest with respect to changes. It is evident that a large number of containers have been moved during this period. Analysis of a selection of sections of the terminal will be discussed separately in the next section.

3.4.1 Analysis of cluster configuration

Two different cluster areas have been analyzed. The SAR image of the same areas is shown for the first and second recording dates in Figure 3.14 and Figure 3.15 for area 1 and 2, respectively. In Figure 3.14 (left), the line labeled A results from wall-ground scattering from the edge of the cluster. The line sections B mark the equal distance interval dI of three less distinct parallel lines to line A. These parallel lines tell that the stacks here are four containers high. The intensity of these lines is weaker than line A, which excludes this being a wall-roof scattering of a stair stack.

Below the lines B, these parallel lines are less pronounced. In contrast to the region above B where we view the containers towards the long sides, the orientation below B is presenting the back short-side of the containers towards the radar. The line C result from a stair as the fourth container is missing at this end of A. The intermediate wall-beam lines are clearly suppressed. From our earlier analysis we would expect a shift in cross-range but that is not observed. The reason is that at the upper end of line A, a lower stack of half-length sized containers (20 foot) is positioned.

At the second recording date in Figure 3.14 (right), a new bright spot has appeared in the upper end. It appears shifted in cross-range relative to line A in the correct direction, indicating a stair

has been established. Detailed analysis shows that it is a double line with different shifting, resulting from two steps. The length of the folded step response is half the line C and we therefore conclude that a step has been formed on the upper 20 foot container part of the cluster. Distances confirm that first there is a double height step followed by the two new single steps. Three 20 foot containers have therefore been added to this cluster.

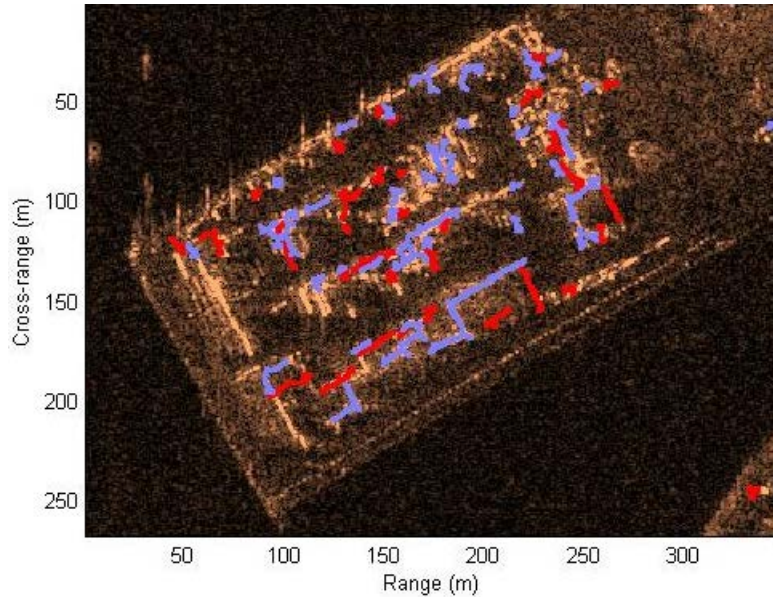


Figure 3.13 Differences in scattered energy between the two days of recording are drawn with blue and red color, respectively.

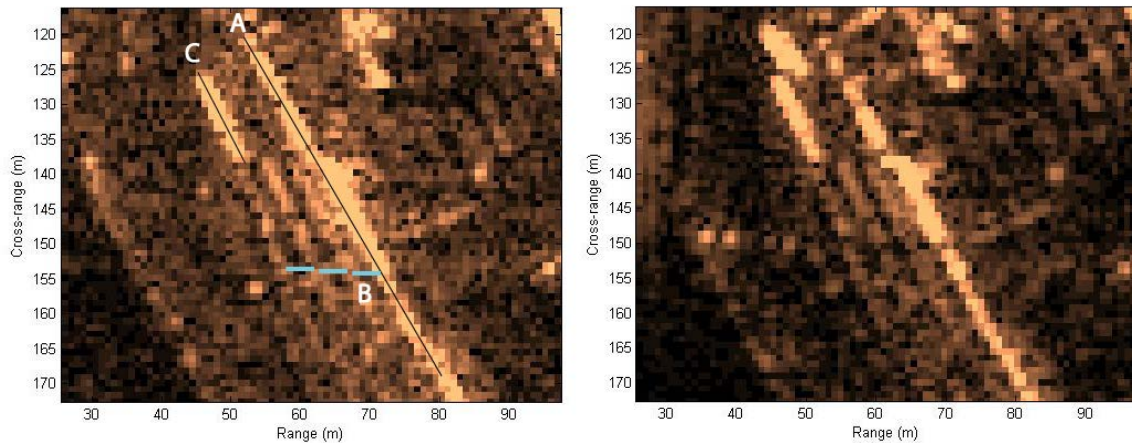


Figure 3.14 Area 1 of the TerraSAR-X SAR image on day 1 and day2 respectively

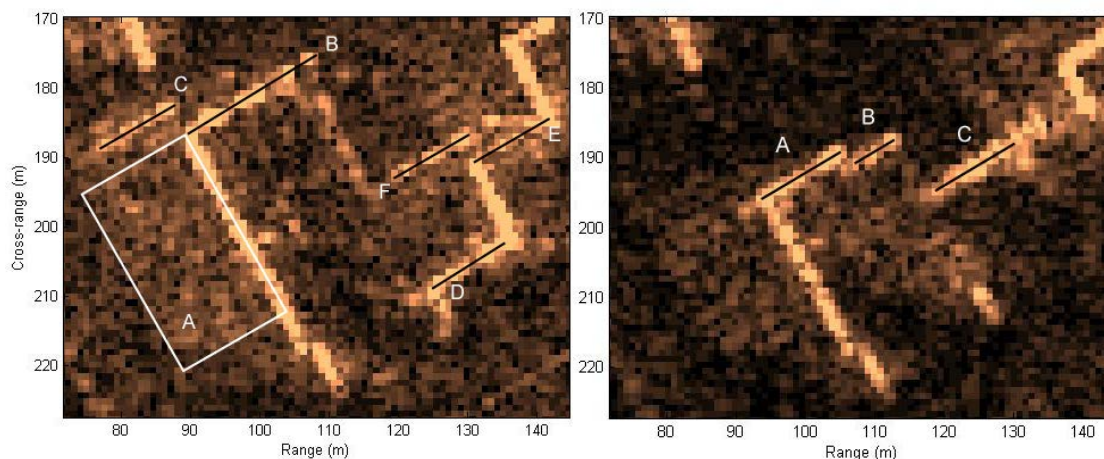


Figure 3.15 Area 2 of the TerraSAR-X SAR image on day 1 and day 2 respectively

In area 2 shown in Figure 3.15 (left), a labeled area A does not show the parallel lines observed in area 1. The reason is that the containers are oriented with the front short side, as shown to the right in Figure 3.16, towards the radar. These sides do not have the same structure or the beam that produce high backscattering levels from the other sides. The wall-ground line in B has a length corresponding to one 40 and one 20 foot container. The folded and shifted 40 foot line in C is generated by a step from height 3 to 4 on the line B stack. The line D is the wall-ground line of a small structure. It is two containers high as observed from ground truth, but this is not possible to tell from the picture. Following the edges we get to the line E which is a wall-ground line of line D's neighboring stack structure. Height is difficult to quantify, but the folded and shifted line in F is a similar step as seen in C leading to the conclusion that there is a total stack height of four.

On the second recording date shown in Figure 3.15 (right), a number of containers have been removed from the end observed as line B on the first day. The new wall-ground lines A and B on the second day represent the 40 and 20 foot container stack sections, respectively. There are no indications of any steps present at this date. From the line D on the first day, containers have been added forming a structure reaching to the new wall-ground line C which puts the stack structure in E on the first day partly in the shadow. The step F, which is still there in the ground truth, is not separable as it coincides with line C.



Figure 3.16 Differences between the front and back short sides of the container

4 Coherent change detection (CCD)

The container terminal under study represented for the NCCD part one instant of container orientation relative to radar (see Figure 4.1 left). To extend this work, coherent change detection has been applied to explore how this additional information helps in analysis and ease of extraction. In addition, an extended coverage of three container terminals that expose containers differently towards the SAR system as shown in Figure 4.1 has been investigated. By doing this, a broader understanding of scattering from stacked container clusters is obtained that add knowledge to SAR analysts and monitoring systems.

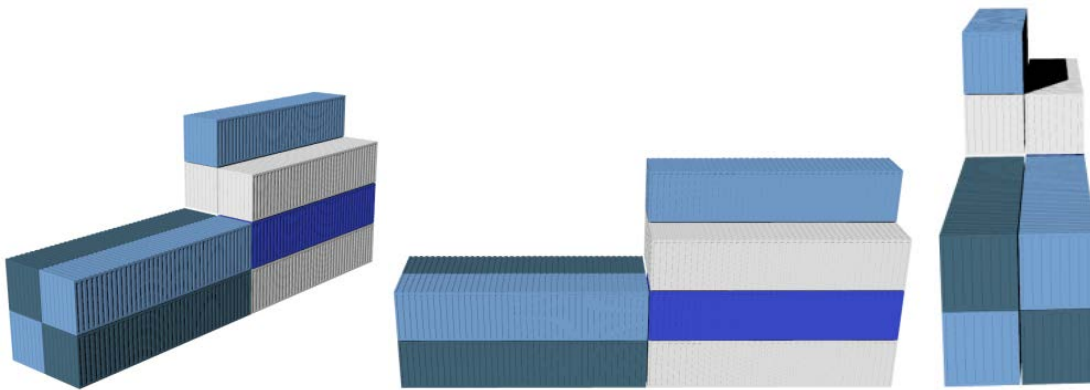


Figure 4.1 Predominant orientation of containers in harbor 1 (left), 2 (middle) and 3 (right) relative to radar, respectively.

A measure of similarity between the complex SAR images has been calculated using the measure of sample coherence (1). The visualization of the sample coherence has been combined with the original images in a color composite image as has been reported with success in earlier work [12].

The scaled images from day 1 and day 2 are displayed in the red (R) and green (G) channels, while the sample coherence $\hat{\gamma}$ value is represented with the blue channel (B) as illustrated to the left in Figure 4.2. Different values in the three channels generate a large span in color variation as is exemplified to the right in this figure for a set of combinations. Using this color coding scheme,

a significant amount of information can be extracted as shown in the sub images of Figure 4.3 to Figure 4.6.

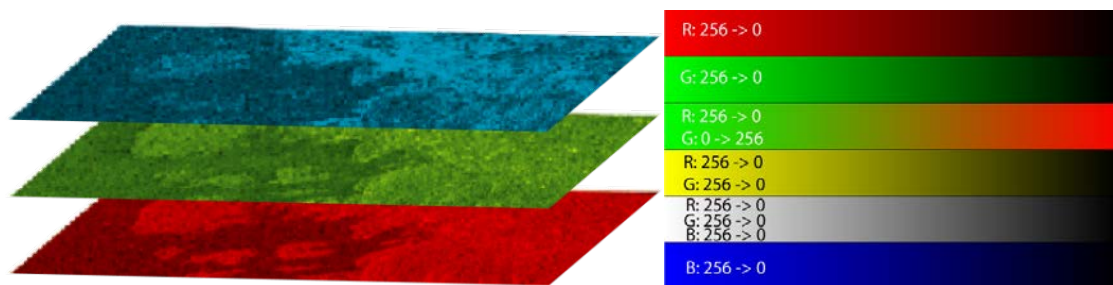


Figure 4.2 Left: Illustration of the three RGB channels of the color composite image containing SAR intensity image from day 1 and 2 and the sample coherence of the two in the upper blue channel. Right: Illustration of resulting colors in the image from combinations of intensities in the three channels.

4.1 Coherent change detection results

To familiarize the reader with how to interpret the image coloring and SAR properties, objects and features observable in these images will be commented on before the container terminals are discussed.

4.1.1 Various objects observed close to the harbor area

As the red and green channels contain the two intensity images, bright red and green represent the presence of an object in either of the days and a lower backscattering value in the other day of those pixels. Since these objects are not fixed in the same pixel, a low sample coherence and low blue content is contributing to the coloring. In the center of the top left image of Figure 4.3, red and green spots appear, resulting from different positioning of trucks and cars as an example of this.

Due to de-correlation in forest and grassy areas from rearrangement of the contributing scattering centers over this time lag of 11 days, low coherence results. The speckle like pattern in such regions results in a mixture of red and green intensities, forming a somewhat natural looking greenish color. This is clearly observed in park and wood landscapes surrounding manmade structures as can be seen around the castle in Oslo in the top right of Figure 4.3. Buildings remain fixed in between recording dates and often have structures that result in high coherence in pixels coinciding with high intensities. These regions are recognized as areas of white towards blue according to intensity and coherence levels. Down town Oslo with its tall houses in the lower left image of Figure 4.3 is a typical example of this where we also observe how tall building experience layover towards the radar located out to the left.

The last image in Figure 4.3 shows hay balls that are coherent in contrast to the surrounding field. This makes them detectable in this color coded image while barely distinguishable in the original images.

These first examples give an introduction to the possibilities of information extraction that is readily available by computing the sample coherence and executing a combined analysis of all three channels.

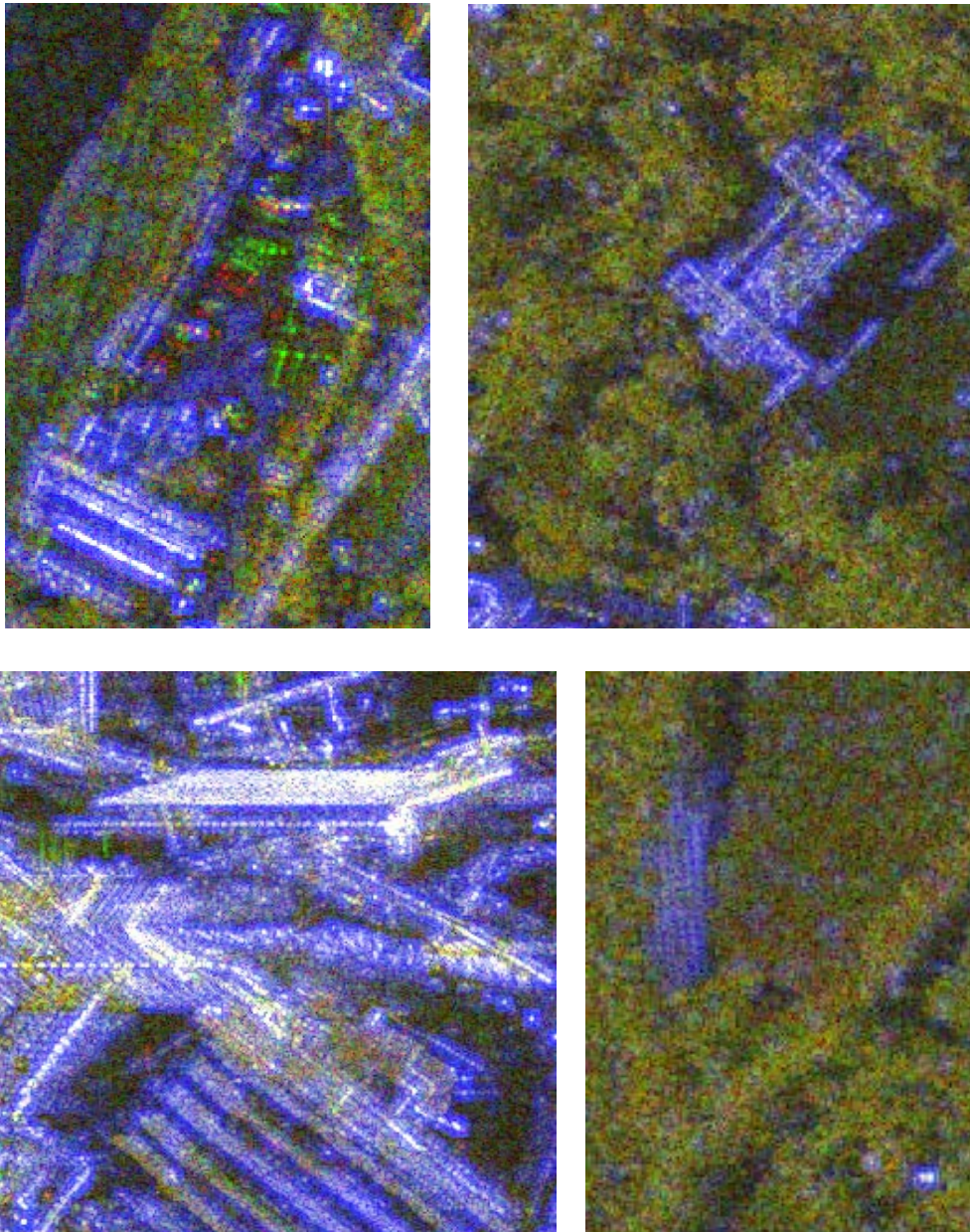


Figure 4.3 Color composite image: From top (a): Different positioning of trucks and cars appear as red and green spots, (b): Wood and park fields with low coherence appear in greenish, (c): High intensity and high coherence from manmade structures of the downtown area, (d): Hay balls with high coherence but an intensity resembling the surrounding field appears clearly.

In living areas in Oslo as shown in the two images in Figure 4.4, parked cars line up along the sides of the streets. In this long 11 days period we observe signs of high activity and high reflectivity spots from either of the two days as well as some that indicates cars left in the same

position. In a shorter time interval changes to a small number of objects would have attracted attention very quickly to interesting locations.

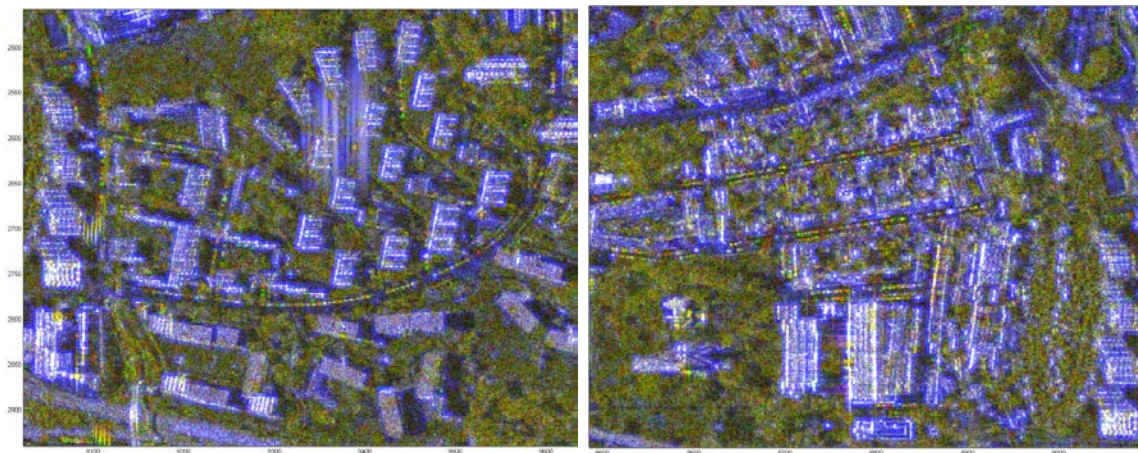


Figure 4.4 Examples where cars parked along the road are clearly visible as colored dots.

More interestingly, in harbor areas, a large range of objects are found that provides information of activity. Cars and trucks are parked in different positions and well defined silhouettes of ships can be extracted for ATR purposes etc. To the left in Figure 4.5, a more or less connected region that appears in yellow is found. Yellow color forms by combining red and green with absence of blue. This part of the quay is a terminal for a large ferry, and this yellow object gives a very good silhouette match with the real ferry when extracted against the background of other colors.

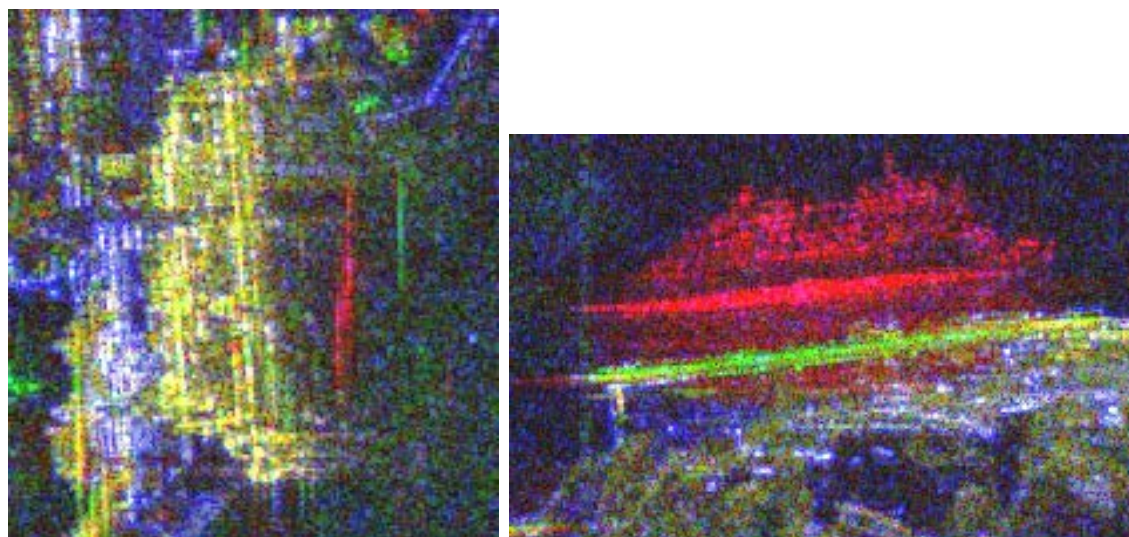


Figure 4.5 Color composite image: (left) Ferry in yellow due to high intensity in both days but low coherence to differences in tide and anchoring, (right) Cruise ship present on day 1 and quay revealed on day 2.

The reason why there is high intensity in red and green channel and at the same time low coherence is that the tide and position of the ship is not exactly the same for the two days. This feature makes it possible to separate it from the rest of the terminal buildings to the left appearing

in more white even though the ship has a layover towards the harbor area. To the right in Figure 4.5, a cruise ship layover forms a clear profile towards the sea foreground on red day (radar to the top). Segmentation of pixels belonging to this ship is straight forward and its result can be used as input to classification software.

In connection with the ferry terminal, vehicles line up waiting for boarding as is observed in the top left image of Figure 4.6. The largest lower region of red, green and yellowish colors represent cars. Individual lines are identifiable and brighter green and red areas at the outskirts represent cars in position on day 1 or 2. The other areas above and to the right consist of trucks as can be estimated by their form factor. These features stand out in contrast to the bright white of infrastructure and buildings nearby. Quantitative measures can be extracted concerning changes in traffic load. The second image to the right in Figure 4.6 represents a building zone in the harbor where the yellow "lines" result from two bounce scattering off a row of long vertical steel beams. To the very right, a red zone indicates presence on day 1. The radar is to the left, and typically when multipath reflections are observed towards a sea surface, cross range spreading is found.

The lower image in Figure 4.6 shows a marina where many boats appear as yellow due to tide variation and differences in exact boat position between the days. High activity on red day (Sunday) is apparent from a filled up parking area to the very right. All these examples show that coherent analysis is a powerful tool that separates a well of objects by coloring and attracts the attention of the analyst.

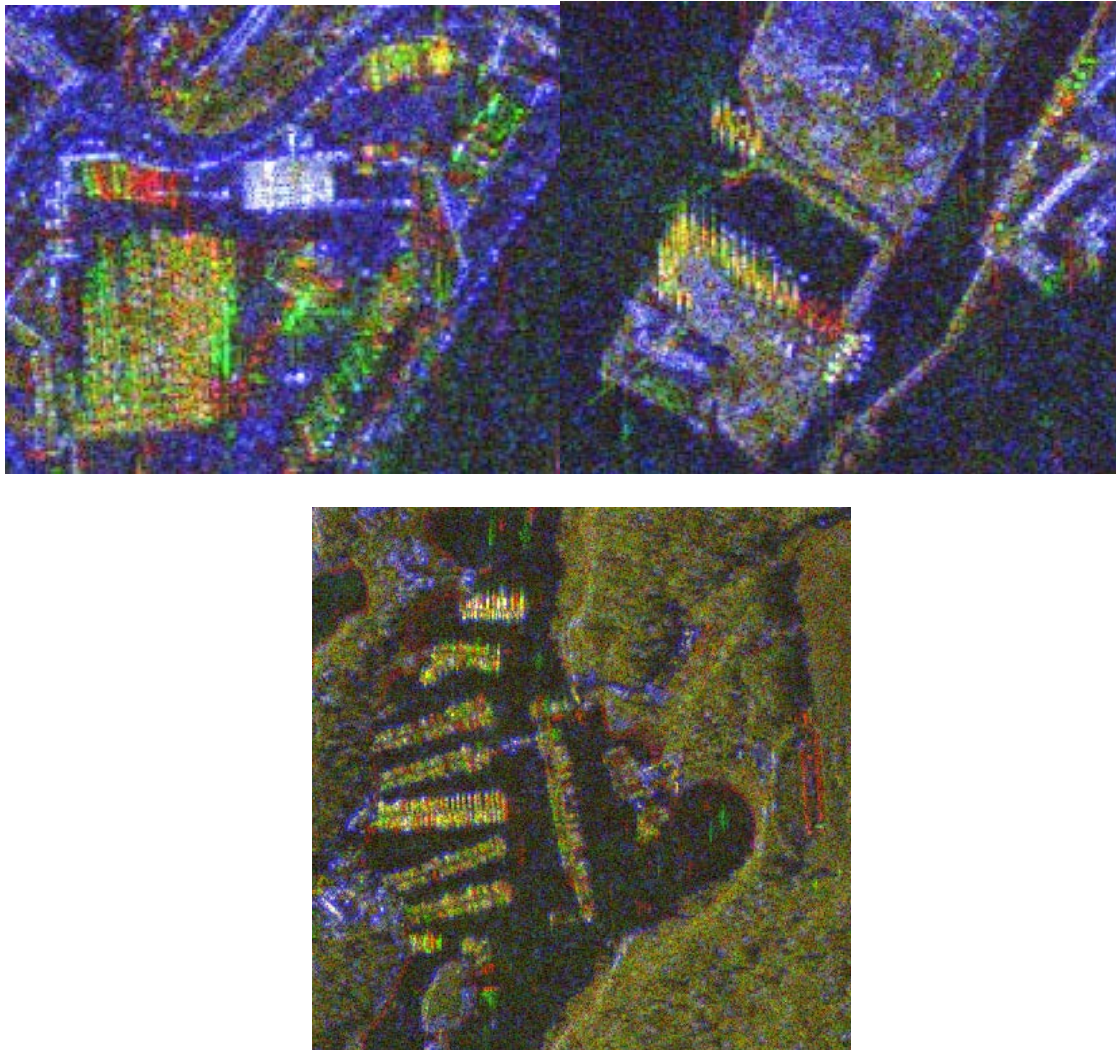


Figure 4.6 Color composite image: Examples from parking space for ferry boarding vehicles, building progress over the time interval and changes in a boat harbor area.

4.1.2 Results from container terminal analysis

From the large number of objects of complex structure that populate harbors, as given a brief overview initially, shipping containers are objects that have a rather simple and regular form. This together with their stacking configuration in tight formation clusters of equally oriented containers enables feature extraction such as stacking configuration, orientation and quantitative measures from SAR images. Three different container terminals have been studied that result in color composite images as shown in Figure 4.7 to Figure 4.9. Changes can to some extent be identified by close inspection of the original images, but by using the coherence in addition more information can be readily extracted. We immediately observe regions where containers have been moved in (green) or out (red) between day 1 and 2, and where no change is found as observed from bright white. In addition some container stacks appear in yellow as was observed for the ferry in Figure 4.5. This represent low coherence but high intensity for both days, which tells us there has been a rearrangement of new containers in approximately same positions but not precisely enough to produce high coherence.

The three terminals represent different geometries where (1) is rotated about 30 degrees from head on relative to the observing SAR sensor, (2) is observed from head on long-side and (3) from head on short-side. The grazing angle to the scene from the radar is approximately 60 degrees.

4.1.2.1 Container terminal 1

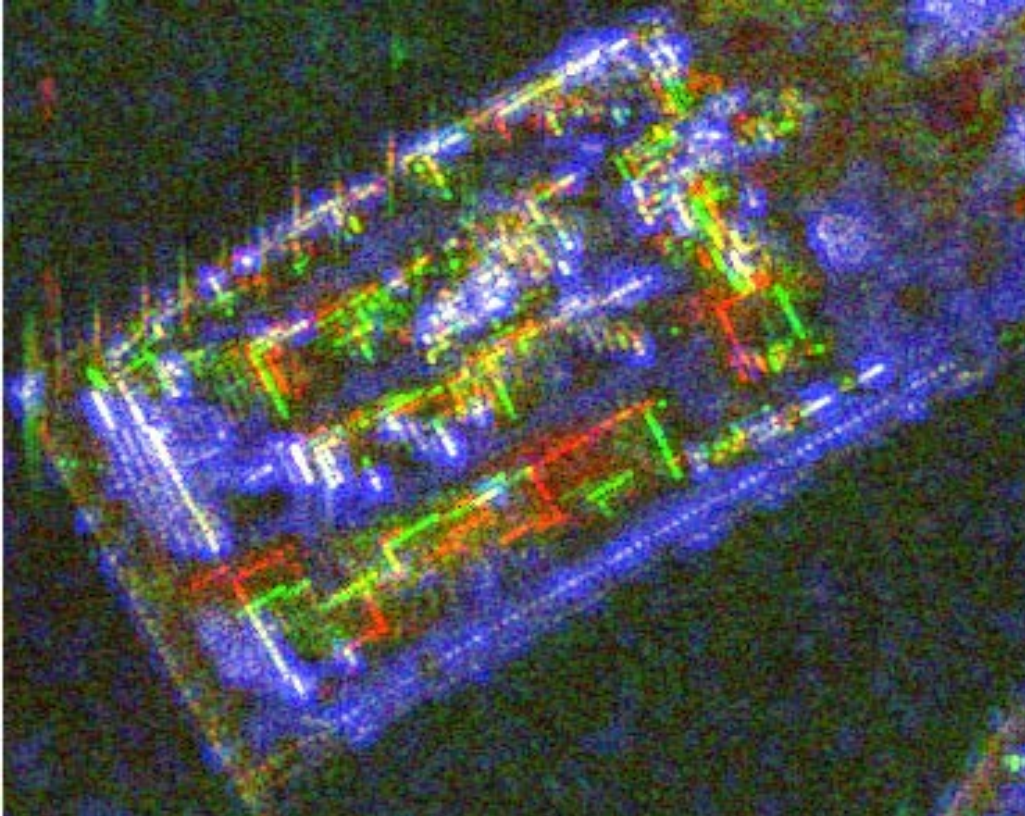


Figure 4.7 Color composite image of terminal 1.

In Figure 4.7, the outline of the sides of the densely packed container clusters towards the radar is observable as bright lines of various lengths resulting mainly from reflections off the bottom beam of the container and the wall above and the wall towards the ground in front of the containers as was found in the non-coherent analysis. Details of fixed and removed container stacks can be quantified by close analysis of the scattering lines. The interior of these clusters are not observable as there are low backscattering from the roof region in this geometry. To have more exact information on the extent of the clusters a second geometry that reveals the shadow sides of the cluster is recommended. In addition, knowledge of terminal equipment such as forklift trucks or other cranes for handling the containers and their limitation in positioning and stacking height helps in calculating the number of containers in the terminal.

4.1.2.2 Container terminal 2

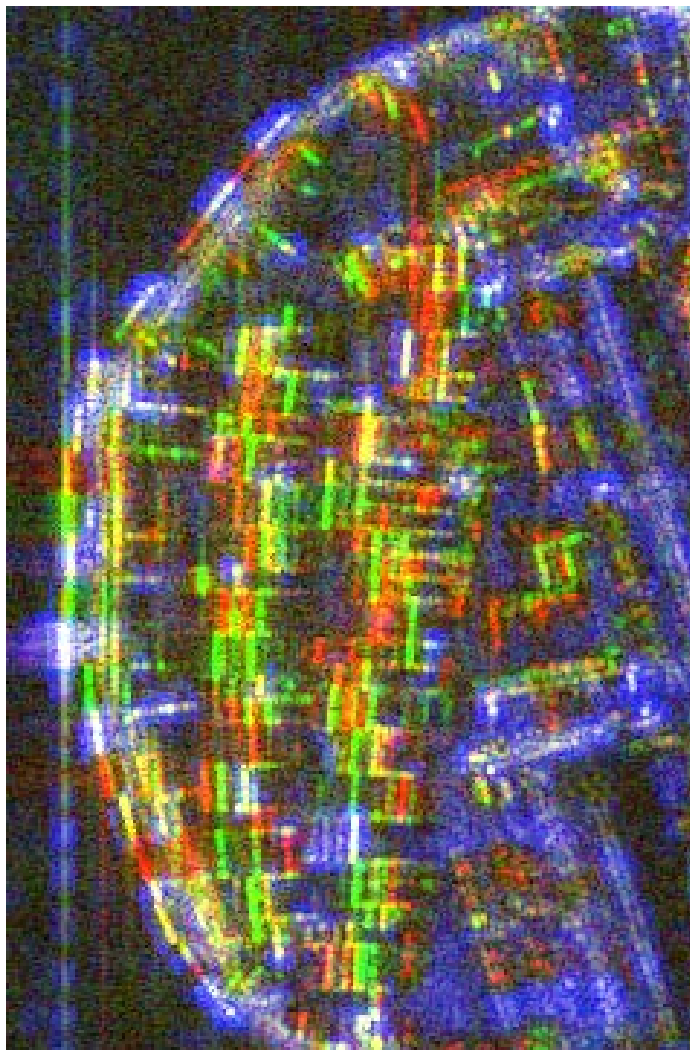


Figure 4.8 Color composite image of container terminal 2.

In the second geometry, Figure 4.8, additional information of the cluster dimension can be extracted from scattering off the side walls in the narrow volume in between stacks. This resulted in stripes that revealed the extension depth of the clusters, which could not be directly observed in previous terminal 1 configuration. If we look at the left column of clusters facing the radar to the left in Figure 4.8, the vertical lines result from scattering of the bottom beam of the containers. We observe a set of parallel lines that result from layover of the stacked containers as explained in the non-coherent analysis. In between these we observe horizontal lines that add information on the number of containers in the horizontal direction of the cluster. The roof regions appear black and do not represent a high level of scattering towards the radar. Analysis on scattering lines that reveals the stacking height combined with the depth can be used to estimate the volume of the container clusters. For the second and third column of clusters the same information can be extracted. We observe that the apparent activity on container rearrangement during an 11 days period in these terminals is major. This suggests that repeated imaging frequency should be adapted to activity level for easier quantification of container rearrangements.

4.1.2.3 Container terminal 3

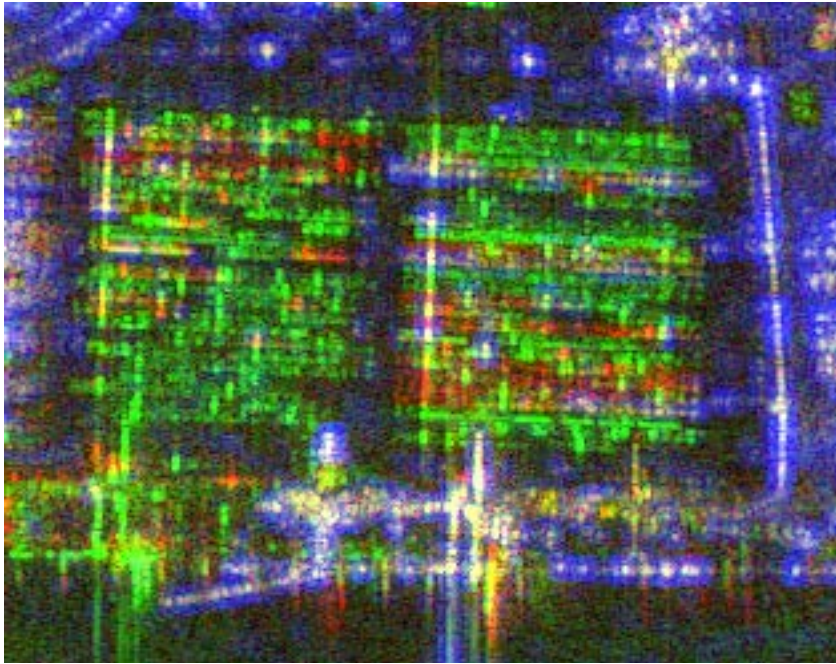


Figure 4.9 Color composite image of container terminal 3.

In the third container terminal in Figure 4.9, containers are viewed towards the short side as shown in the right of Figure 4.1. While the two first terminals handle containers with container handlers on wheel that has a maximum stacking height of four and restrict access to containers to the ones on the cluster perimeter, this third terminal are equipped with straddle carriers that moves over the container stacks of maximum height three and can therefore store containers more densely and access all containers from the top of the stacks. This result in a quite different storing geometry relative two the two previous terminals.

The ribbed pattern of the roofs generates high backscattering values in this geometry due to the forming of two-bounce dihedrals. This result in an image where the whole container roof becomes visible and consequently contributes to the coverage estimates of the cluster. Information of the cluster area coverage is readily extractable as can be seen in the image. Two square areas are used for container storage. We observe connected regions in red and green representing containers on the two days. To the left in both square regions we observe a vertical line that has a stronger backscatter. This represents the scattering of the end wall towards the ground and identifies the start position of the cluster. Scattering response to the left of this results from containers on higher levels in the stack and knowledge of container height and viewing geometry allow estimates of container stack height. The number of containers in the horizontal direction can be calculated from pixel size of the image and assumed container length. The exact stacking height along each row is difficult to observe and therefore we cannot calculate the number of containers in the cluster of this terminal.

5 Conclusions

The most predominant scattering regions of a container stack are found to originate from wall-beam, wall-ground and wall-roof regions. Their backscattering characteristics have been shown from CAD models of containers and simulations of the SAR response using MOCEM LT. Simple stack and step structures of containers have been used to learn to interpret differences between stacked containers, stairs and combinations of the two. This knowledge has been used to determine stack height and structure from SAR images recorded at two different dates. An automatic change detection scheme has been applied to the two SAR images directing attention and further detailed analysis towards detected areas of major change. The use of a simulation tool is a valuable aid for a human analyst to quickly address in detail the scattering response from different combinations of container CAD model clusters for comparison towards an original SAR image.

The use of coherent change detection with high fidelity co-registered SAR images and visualization using color composite images where the two intensity images and the sample coherence constitute the three image channels (RGB) have been shown for container terminals and other objects in the harbor area. The use of coherence between complex SAR images gives additional information compared with the intensity images that represents a powerful tool for segmentation and extraction of various objects and focus attention to areas of activity due to the coloring scheme. The analysis of the three container terminals has provided knowledge of quantitative measures that can be found in such data as a function of view geometry as well as insight in limits. Prior knowledge of the container handling equipment of the terminals provides information that can be used in extracting number of containers in individual clusters and changes observed over the time interval of two such recordings. A registration interval of 11 days resulted in detected changes that in some areas could be too high to extract reliable measures and future scheduling of recordings should adapt to expected activity level for the area of interest.

Referenses

- [1] A. J. Bennett and D. Blacknell, "The extraction of building dimensions from high resolution SAR imagery", Radar 2003, Sept. 3-5, 2003.
- [2] D. Blacknell, R. D. Hill and C. P. Moate, "Analysis of Building Dimension Estimation Accuracy from SAR Shadow Information", 2008, June 2-5, 2008.
- [3] . G. White, "Change detection in SAR imagery", Int. J. of Remote Sensing, vol. 12, nr 2, pp. 339-360, 1991.
- [4] A. C. Van den Broek and R. J. Dekker, "Evaluation of high resolution space borne SAR for man-made target characterization", EUSAR 2008, June 2-5, 2008.
- [5] A. Thiele et. al., "Building recognition fusing multi-aspect high-resolution interferometric SAR data", IGARSS 2006, vol. 7, nr 31, pp. 3643-3646, 2006.
- [6] D. Pastina, G. Battistello and A. Aprile., "Change detection based GMTI on single channel SAR images", EUSAR 2008, June 2 – 5, 2008.
- [7] D. Cristallini and P. Lombardo, "Detection of step changes in a long sequence of SAR images", EUSAR 2008, June 2 – 5, 2008.
- [8] C. Cochin et.al., "MOCEM – An 'all in one' tool to simulate SAR image", EUSAR 2008, June 2-5, 2008.
- [9] E. F. Knott et. al., "Radar Cross Section", Artech House, 1985.
- [10] T. Johnsen, "Change detection and detailed analysis of stacking configuration of containers in TerraSAR-X SAR images", Radar Conf. 2010 IEEE, Washington DC, 2010.
- [11] M. Preiss and N.J.S. Stacy, "Coherent Change Detection: Theoretical Description and Experimental Results", Technical Report, DSTO-TR-1851, August, 2006.
- [12] P. Wright, T. Macklin, C. Willis and T. Rye, "Coherent Change Detection with SAR", 2nd EMRS DTC Technical Conference, Edinburgh, UK, 2005.